JOURNAL OF MATERIALS SCIENCE 15 (1980) 1547–1556

The effect of pressure on the melting temperature and lamellar thickness of trans-1,4-polyisoprene crystallized at pressures of 1 bar to 3 kbar

C. K. L. DAVIES, M. C. M. CUCARELLA*
Department of Materials, Queen Mary College, Mile End Road, London E1 4NS, UK

The melting temperatures of both low-melting form and high-melting form trans-1,4-polyisoprene crystals grown at 1 bar pressure have been determined as a function of pressure. Equilibrium melting temperatures have been determined for specimens crystallized at pressure. All the melting temperatures increase by approximately 15 K kbar^{-1}. Lamellar thicknesses have been measured by both thin film transmission electron microscopy and via low-angle X-ray studies over the pressure range 1 bar to 3.0 kbar. The two methods of measurements give good agreement. Crystals of a given thickness melt at a given temperature, at 1 bar pressure, independent of temperature or pressure of crystallization. Crystals of a given thickness are formed at a given supercooling independent of the pressure of crystallization. At a given crystallization temperature the thickness of crystals formed decreases with increasing pressure. Crystals of the same form grow, at all pressures studied, by the same basic mechanism. Chain-extended type crystals were not formed.

1. Introduction

Many studies have been carried out on the effect of pressure on the crystal melting temperatures of crystals grown at or near atmospheric pressure using either dilatometry [1–8, 12, 13, 16, 18] or differential thermal analysis [4, 9–11, 14, 15]. The majority of polymers exhibit an increase of melting temperature (T_m) with pressure of between 10 and 30 K kbar^{-1}; the value of dT_m/dP_m tending to decrease with increasing pressure. The majority of polymers also exhibit a continuous decrease in the molar volume change (ΔV_m) on melting with increasing pressure [1, 7–9, 16]. Using the Clausius–Clapeyron equation

$$\frac{dP_m}{dT_m} = \frac{\Delta S_m}{\Delta V_m} = \frac{\Delta H_m}{T_m(\Delta V_m)}, \quad (1)$$

approximate values of the entropy change (ΔS_m) and the enthalpy change (ΔH_m) as a function of pressure can be calculated [19]. Care must be taken in interpretation of these data as in some cases structural changes (phase changes or crystal thickening) are known to occur prior to melting at pressure. In the case of penton crystals [1] a pronounced minimum in both ΔS_m and ΔH_m is observed which is almost certainly the result of a phase change. Polypropylene [1] and non-branched polyethylene [1, 8, 9] show increases in both ΔS_m and ΔH_m. In the case of polypropylene this may result from a phase change [20] and in polyethylene the increase may be due to crystal thickening [11]. Branched polyethylene shows little change in either ΔS_m or ΔH_m as a function of pressure and polyethylene oxide shows a considerable decrease in both. In all cases ΔH_m changes by less than a factor of 2 over the pressure range 1 bar to 3 kbar [19]. However, neither the magnitude nor the sense of the changes can be unambiguously interpreted.

A great deal of work has been carried out on

*Present address: Escuela de Ingenleria Metalurgica y ciencia de los Materials, U.C.V. Apartado 51717, Caracas, Venezuela.

0022–2461/80/061547–10$03–00/0

the crystallization and annealing behaviour at pressure of polyethylene [7–11, 21–24] and nylons [18, 25]. Lamellar crystals are known to thicken in these materials at atmospheric pressure and the process is accelerated by annealing at elevated pressures. Crystallization at pressure in these materials, produces thick chain extended type crystals and, under certain circumstances, chain-extended crystals. Chain-extended crystals may nucleate separately, grow from folded chain crystals or nucleate via a new phase.

The change in crystal thickness has been studied by small-angle X-ray scattering and by observations of electron micrographs of fractured specimens. It is not clear why crystals thicken or are nucleated in a thick form at elevated pressures. The increase in crystal thickness with increasing pressure usually results in an increase of crystal perfection, melting temperature (T_m) and melting enthalpy (ΔH_m). These increases in T_m and ΔH_m should, however, be clearly distinguished from the changes which occur at pressure for the melting of a given crystal formed at various pressures.

While many studies appear in the literature on the effect of pressure on polymer crystal morphology, few studies appear on the effect of pressure on kinetics of crystallization [26, 27]. These require the ability to follow the crystallization process as a function of temperature and time at a given pressure or the ability to stop crystallization at a given time while the specimen is under pressure.

The present work is part of a study of the kinetics of crystallization of trans-1,4-polyisoprene (TPI) at pressures up to 3.0 kbar. The polymer was chosen for this study as the crystals are not known to thicken considerably at atmospheric pressure and as a result its behaviour may be different from that of polyethylene or nylons, particularly at relatively low pressure. Furthermore, as thickening may be slow, it should be possible to unambiguously distinguish between changes in melting temperature resulting directly from the applied pressure and those resulting from changes in crystal thickness. It is possible in this polymer, to stop crystallization at a given time at pressure by reacting the unsaturated polymer with osmium tetroxide vapour and if crystallization is carried out in thin films it is possible to measure the crystal thickness resulting from crystallization at any pressure by transmission electron microscopy. It also becomes possible to determine spherulite growth rates at pressure. Studies of this type have been carried out on TPI at atmospheric pressure and both the morphology and kinetics of crystallization are well documented [28, 29]. This polymer crystallizes in two forms; low-melting form (LMF) and high-melting form (HMF) with equilibrium melting temperatures of 78 and 87° C [30]. LMF spherulites contain only crystals with an orthorhombic unit cell and HMF spherulites crystals with a monoclinic unit cell [28, 31, 32].

The present paper reports on the variation of melting temperature, at atmospheric pressure, of crystals grown at various pressures and on the variation of melting temperature, as a function of pressure, for crystals grown at various pressures, including atmospheric pressure. Lamellar crystal thicknesses have been measured by transmission electron microscopy with a limited number of measurements from low-angle X-ray scattering data. The aim of the study was to follow the change of lamellar thickness and melting temperature as a function of pressure and to determine whether significant changes of crystal thickness and perfection occurred, at pressure, for a polymer in which crystals are not known to thicken considerably at atmospheric pressure.

2. Experimental details

2.1. Materials

The trans-1,4-polyisoprene was prepared by purification of a commercial grade of gutta percha* by solution and reprecipitation [28]. Thin films for transmission electron microscopy, 100 nm thick, were prepared on a water surface from a 1% solution in benzene as reported previously [28]. Some films were strained prior to crystallization using the method devised by Andrews [28, 33]. All films were melted at pressure prior to crystallization. The molecular weight ($\bar{M}_N$) of the melted sample was 3.0×10^4.

2.2. High-pressure apparatus

The high-pressure system was originally constructed by Edwards and Phillips [34] and was based on a design described by Crawford [35]. Details of the modified apparatus are given elsewhere [19]. The pressure is generated by a two-stage intensification of the pressurizing medium, which in the present study is high-purity argon

*Supplied by Penfold Golf Ball Ltd, Birmingham, UK.

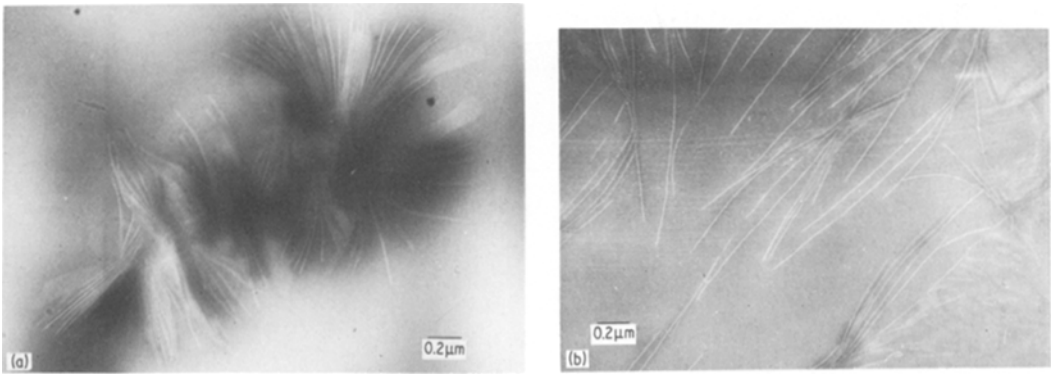

Figure 1 Electron micrographs of lamellar crystals. (a) Strained 50% and crystallized for 1 h at 40° C and 2 kbar pressure. (b) Crystallized for 2 h at 68° C and 1 kbar pressure.

gas. The first stage intensification is carried out by a gas pump operated via a standard compressed air line. The final pressure is achieved by a high pressure intensifier operated by means of a compressed air-driven oil pump. The pressure was determined by following the change in resistance of a manganin coil with pressure, which was built into the system. The crystallization vessel can be operated at pressures up to 3.5 kbar and the high-pressure DTA cell up to pressure of 2.0 kbar. The crystallization bomb was fitted with a plug which enabled crystallization to be terminated at any time, at pressure, by staining the sample with osmium tetroxide vapour.

2.3. Measurement of lamellar thickness

The lamellar thickness was determined by both transmission electron microscopy (L_E) and via long-period measurements from low-angle X-ray scattering (L_X).

The electron microscope measurements were made from photographic plates of either spherulitic structures (Fig. 1a), or row nucleated structures (Fig. 1b) in strained films. Thin films strained from 0 to 150% prior to crystallization were used for this study. In each case the width of the thinnest lamella was determined from electron microscope plates, for each crystallization temperature at each pressure, using a microdensitometer. LMF and HMF crystals could be distinguished by the large differences in crystal length due to differences in growth rate at a given temperature or by electron diffraction experiments [28, 29]. Even if the staining technique accurately images the 'crystal thickness' there are difficulties in using this technique particularly for very thin images [36] as a result of the limit

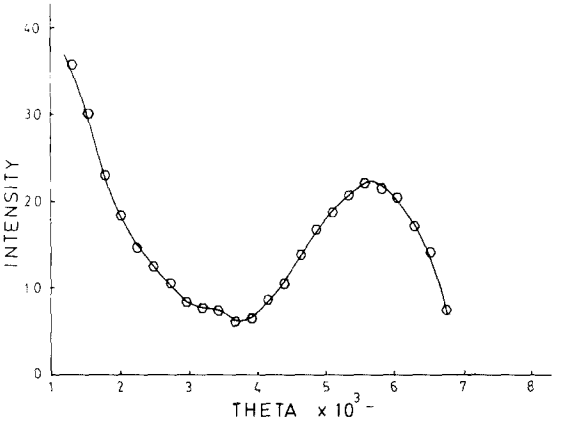

Figure 2 Desmeared and Lorentz corrected X-ray intensity distribution curve from a specimen crystallized at 65° C and 3 kbar pressure.

of resolution of the optical system when two changes of contrast lines are close together. In the present case, estimates of the spread of the image using a Cauchy analysis, as proposed by White [36], have been made and lead to a maximum error in the measured thickness of 2% at 10 nm which increases to 8% at 5 nm. In the present work the as-measured results for lamellar thickness are reported.

The long period was measured using a Kratky low-angle X-ray camera. An example of a desmeared [37] and Lorentz [38] corrected intensity distribution curve is shown in Fig. 2. A pronounced first-order intensity maxima is clearly visible from which an 'average value' of the long period was calculated. Low-angle X-ray studies were carried out at atmospheric pressure on fully crystallized specimens. Only data obtained from specimens which contained a large majority of either HMF

or LMF TPI crystals was used to calculate the lamellar thickness. The linear crystallinity was estimated from the wide-angle X-ray scattering curves, from fully crystallized specimens, using the method proposed by Natta *et al.* [39]. A crystallinity near to 40% was determined for all specimens crystallized at atmospheric pressure and a similar value for the few specimens studied, which had been crystallized at higher pressures. The lamellar thickness (L_X) was determined from the long period by simple multiplication by the linear crystallinity. The lamellar thickness (L_X) values may, therefore, be subject to error and the main justification for their inclusion in this paper is as a basic comparison with the much more extensive determination of lamellar thickness (L_E) from electron microscopy. This is deemed significant, as measurements of both types, determined on a given polymer under the same conditions of crystallization, have not been reported previously.

2.4. Melting temperatures

Melting temperatures at atmospheric pressure were determined using a DuPont 900 thermal analyser and at high pressure using the high-pressure DTA cell. In both cases a heating rate of 15 K min^{-1} was used.

In a large number of specimens, only LMF or HMF crystals are present and a single melting peak is observed. In some specimens two peaks are observed corresponding to LMF and HMF crystal melting temperatures. In both cases the crystal melting temperatures were taken to be the peak temperatures as measured from the DTA curves. Some atmospheric pressure DTA curves were discarded as it was apparent that the specimen had not fully crystallized at pressure and further crystallization had occurred at an unknown lower temperature and pressure, resulting in further peaks.

The DTA measurements at atmospheric pressure produced reliable heats of melting but the base line variation on curves obtained from the high-pressure DTA cell did not allow accurate measurements of the heats of melting at pressure.

3. Experimental results and discussion

3.1. Melting temperatures

Figs. 3a and b show the melting temperature (T_m) as a function of pressure for a given crystallization temperature, for specimens crystallized at atmospheric pressure. The melting temperature increases linearly by approximately 15 K $kbar^{-1}$ for both HMF and LMF TPI crystals for all crystallization temperatures. This increase is very similar to that measured for nylon-6 ([18] p. 654) where a linear increase of 16 K $kbar^{-1}$ was observed over a similar range of pressures. If no crystal thickening occurs on heating to the melting temperature at pressure, then this increase in melting temperature with increasing pressure, for a given crystal thickness and degree of perfection, can be solely attributed to the change in the thermodynamic parameters of the system as a function of pressure.

Fig. 4 shows plots of T_m versus T_c for TPI crystallized at 2 kbar. Curve 1 is for specimens melted at atmospheric pressure and curve 2 for specimens melted at a pressure of 2 kbar. It can be seen that the lines are parallel with a melting temperature difference of approximately 15 K $kbar^{-1}$. The increase in melting temperature with increasing crystallization temperature is exactly the same at pressures of 2 kbar and 1 bar. Further-

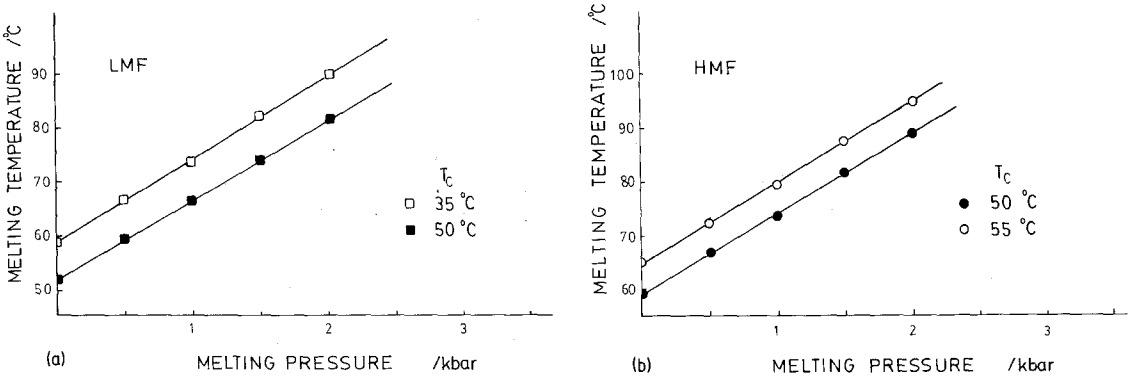

Figure 3 The melting temperature (T_c) as a function of pressure for a given crystallization temperature: (a) LMF crystals, (b) HMF crystals.

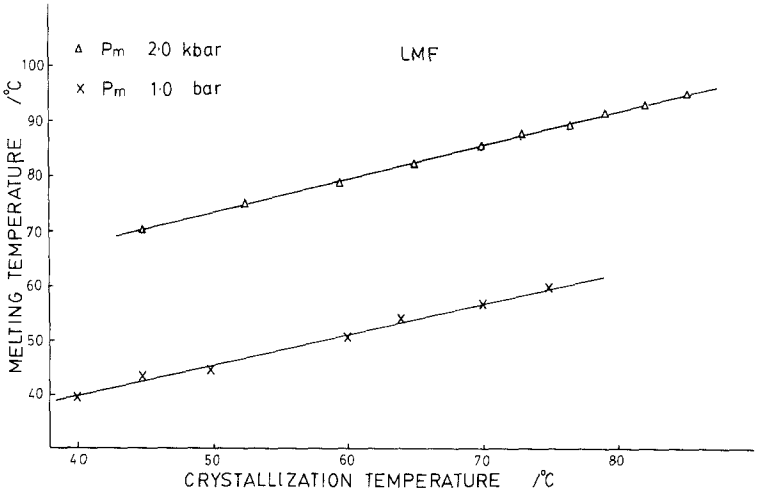

Figure 4 The melting temperature (T_m) as a function of crystallization temperature (T_c) for TPI crystallized at 2 kbar. Curve 2 is for specimens melted at 1 bar pressure and curve 2 for specimens melted at 2 kbar pressure.

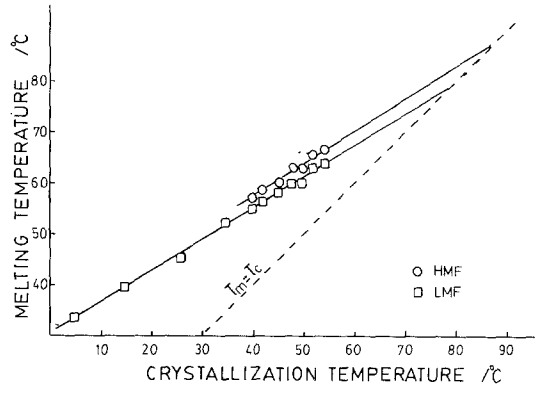

Figure 5 The melting temperature (T_m) as a function of crystallization temperature (T_c) for TPI crystallized and melted at atmospheric pressure.

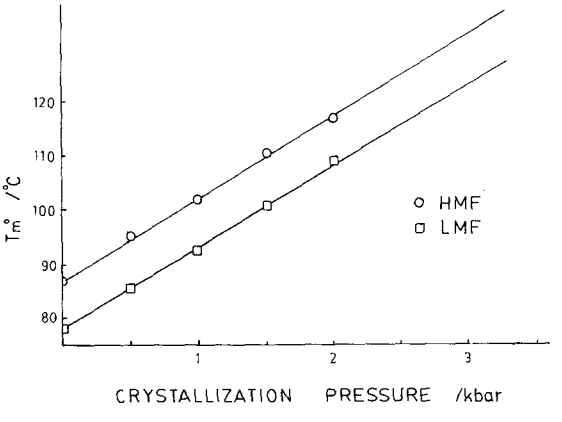

Figure 6 The equilibrium melting temperature (T_m^0) as a function of pressure.

more, the increase in melting temperature with increasing melting pressure for samples crystallized at 2 kbar is 15 K kbar^{-1} as it was for specimens crystallized at a pressure of 1 bar.

Fig. 5 shows the melting temperature as a function of crystallization temperature for TPI crystallized at atmospheric pressure and melted at atmospheric pressure. Comparison of melting points of samples crystallized at a given temperature, at 1 bar and 2 kbar pressure (Figs. 4 and 5) and melted at 1 bar pressure shows a decrease in melting temperature of approximately 15 K kbar^{-1}. This suggests an increase in the equilibrium melting temperature of approximately 15 K kbar^{-1}. The extrapolation of these curves (Fig. 5) to the line $T_m = T_c$ using a least-squares analysis yields equilibrium melting temperatures of 87.0 ± 1.3° C and 78.1 ± 1.1° C for HMF and LMF crystals, respectively. These values agree closely with those reported by Lovering and Wooden [30]. Equilibrium melting temperatures for samples crystallized and melted at a given pressure have been determined similarly using data of the type shown in Fig. 4. The equilibrium melting temperature is plotted as a function of pressure in Fig. 6 and both crystal forms show an approximate increase of 15 K kbar^{-1}. The increase in the equilibrium melting temperature with increasing crystallization pressure corresponds exactly in magnitude to the increase in melting temperature with increasing pressure for samples crystallized at a given pressure. The major effect of pressure, at least in the range 1 bar to 2 kbar, would seem to be to increase the equilibrium melting temperature as a direct result of pressure on the thermodynamic parameters of the system rather than indirectly via crystal thickening or increase in crystal perfection.

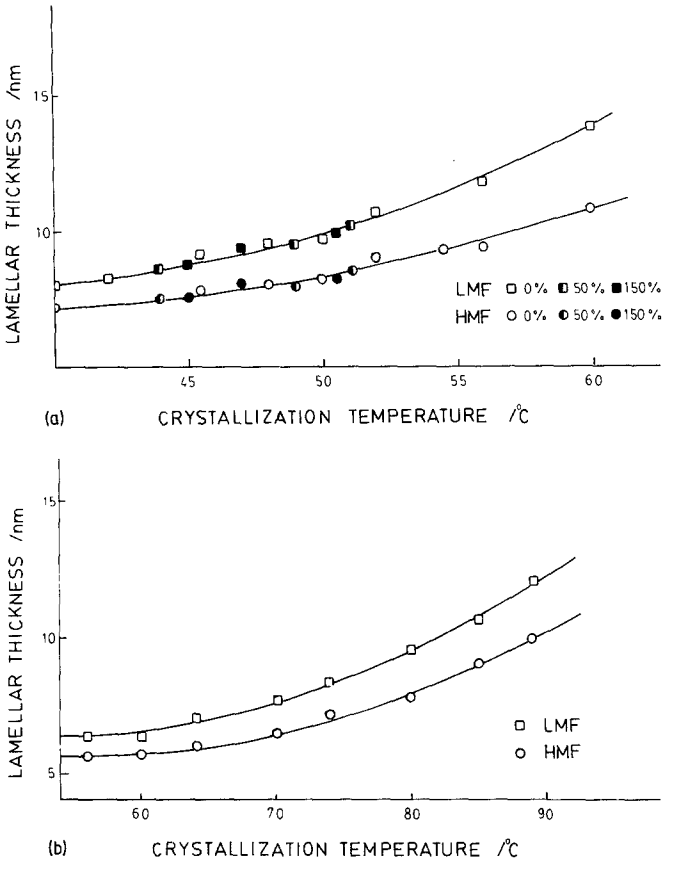

Figure 7 The variation of lamellar thickness (L_E) with crystallization temperature (T_c). (a) Specimens crystallized at 1 bar and strained 0, 50 or 150% prior to crystallization. (b) specimens crystallized at 2.5 kbar.

3.2. Lamellar thickness data

Figs. 7a and b show plots of the variation of lamellar thickness (L_E) with crystallization temperature at pressures of 1 bar and 2.5 kbar. At all pressures the lamellar thickness decreases with decreasing crystallization temperature and LMF crystals are always thicker than HMF crystals. In Fig. 7a, lamellar thickness values for specimens strained 0, 50 and 150% are shown. There appears to be no effect of prior strain on the lamellar thickness developed during subsequent crystallization. This is not surprising as the strain is almost certainly relaxed prior to lamellar crystallization. The variation of the lamellar thickness (L_E) with pressure is shown for LMF and HMF crystals in Figs. 8a and b. It can be seen that the lamellar thickness decreases with increasing pressure at a given crystallization temperature, at all pressures up to 3 kbar. Thick chain-extended type crystals do not form in TPI at pressures below 3 kbar. Figs. 9a and b show the lamellar thickness plotted as a function of the supercooling (ΔT). Both the electron microscope data (L_E) and the lamellar thickness data from long-period measurements (L_X) are included. Lamellar thicknesses are included from both sides of the maxima in the growth-rate temperature curve. These data are not normally attainable for TPI as it is not possible to temperature-quench specimens through the maxima at atmospheric pressure. However, as the maximum growth rate and nucleation rate decreases rapidly with increasing pressure [40] it is possible to quench a specimen at a pressure of 3 kbar to any other temperature through the maxima at 3 kbar. The pressure can then be lowered to any value and the specimen crystallized at the new temperature and pressure. It is difficult to maintain thin film coherency during this pressure-quenching step and most of the lamellar thickness data for low-temperature, low-pressure crystallization is derived from the long-period measurements (Fig. 9a) rather than from electron microscope measurements. In the case of high-pressure crystallization, lamellar thickness data are available from both sources over the whole temperature range (Fig. 9b). The agreement between the measurements from the two sources is very good. This may be rather fortuitous as the electron

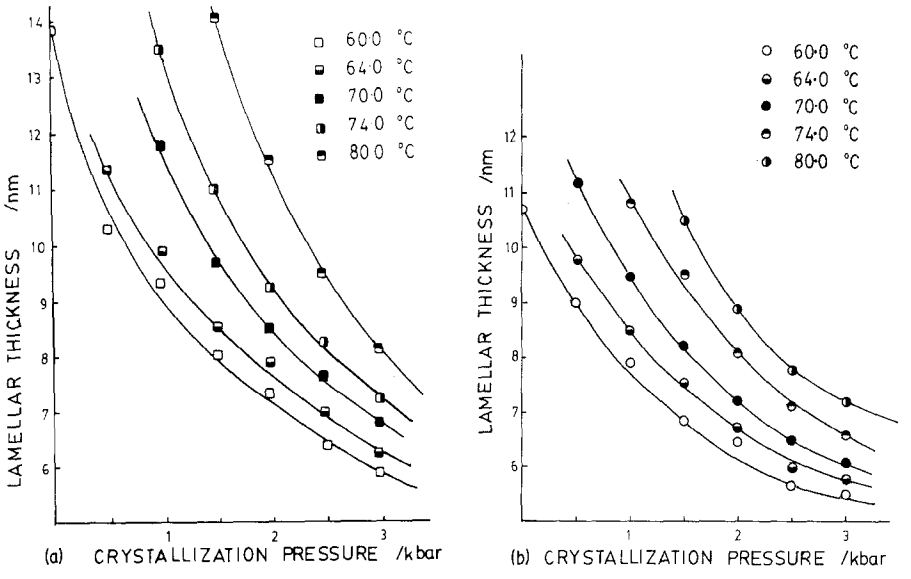

Figure 8 The variation of lamellar thickness (L_E) with pressure for a given crystallization temperature: (a) LMF crystals, (b) HMF crystals.

microscope lamellar thickness is a minimum value and the long-period lamellar thickness an "average" value subject to the uncertainty discussed earlier. It can be seen from Figs. 9a and b that a given lamellar thickness is obtained at a given supercooling independent of pressure of crystallization for both HMF and LMF crystals.

Fig. 10 shows the reciprocal of the lamellar thickness plotted as a function of crystal melting temperature, measured at atmospheric pressure. Some data points have been excluded as they superimpose on those plotted. It can be seen that crystals of a given thickness melt at a given temperature independent of temperature or pressure of crystallization. This suggests that crystals of the same form are obtained at pressures up to 3 kbar and that no significant thickening occurs.

The secondary nucleation theory of polymer crystallization represents the lamellar thickness of polymer crystals as a function of supercooling ΔT by an equation of the form [41, 42],

$$L = \frac{2\sigma_e T_m^0}{\Delta H_m \Delta T} + \delta l$$

where σ_e is the fold surface energy, and ΔH_m is the enthalpy of melting. If the terms within δl are small, the lamellar thickness should be linearly related to the ratio of the equilibrium melting temperature (T_m^0) and the supercooling (ΔT). The lamellar thickness is plotted as a function of $T_m^0/\Delta T$ in Fig. 11. The data obtained at crystallization pressures of 0.5, 1.5, 2.5 kbar is excluded as are some data points from the other pressures as the points superimposed on those plotted. The equilibrium melting temperatures, measured at pressure, are used for pressures up to 2.0 kbar. The values of the equilibrium melting temperatures at a pressure of 3.0 kbar are determined by extrapolation of the plots in Fig. 6. It can be seen that the data for all pressures, for both HMF and LMF crystals fall close to the same line. The ratio $\sigma_e/\Delta H_m$ is, therefore, nearly independent of pressure and equal for both crystal forms. This suggests that the effect of pressure is only to increase the equilibrium melting temperature and that crystals of the same form growing by the same basic mechanism occur at all pressures up to 3.0 kbar with little thickening.

If the melting enthalpy (ΔH_m) as a function of pressure were known it would be possible to calculate the surface energy σ_e. It should be noted that the ΔH_m required in this case, is that resulting directly from the effect of pressure on the melting of crystals via the Clausius–Clapeyron equation as no significant increase in ΔH_m is anticipated due to crystal thickening or increase in crystal perfection. Unfortunately, no reliable molar volume changes (V_m) are available and hence an accurate calculation is not possible at this time. It is not even possible to guess at the sense of the

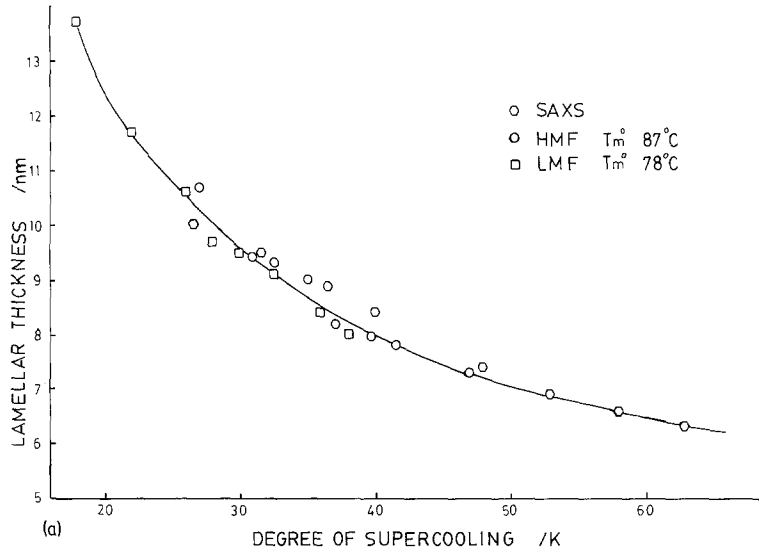

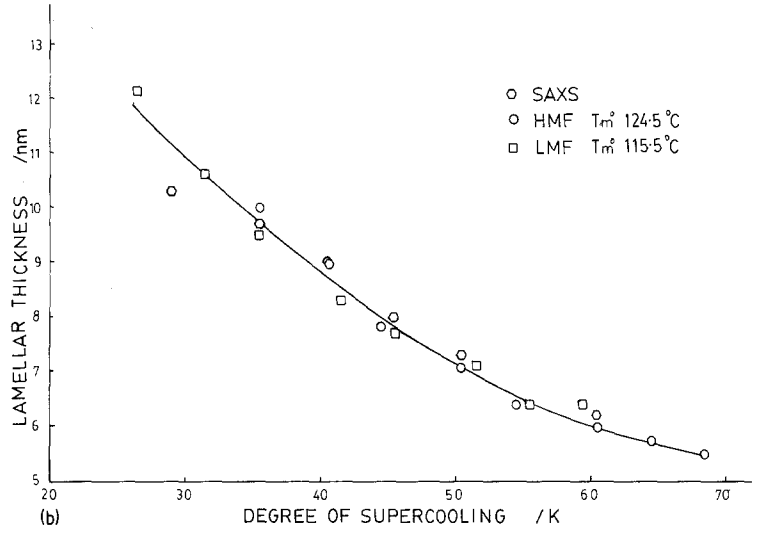

Figure 9 The variation of the lamellar thickness, measured by electron microscopy (L_E) and that measured from the X-ray long period (L_X) with supercooling (ΔT): (a) 1 bar pressure, (b) 3 kbar pressure.

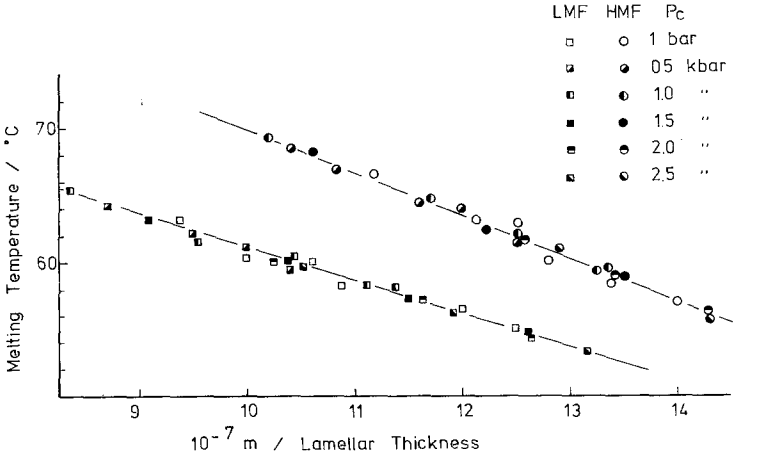

Figure 10 The reciprocal of the lamellar thickness as a function of the crystal melting temperature, measured at 1 bar pressure.

TABLE I Values of σ_e for LMF and HMF trans-polyisoprene crystals

Reference	Method	σ_e(J m^{-2})	
		HMF	LMF
[29]	Lamellar thickness from thin film electron microscopy melt-grown	60.1×10^{-3}	45.1×10^{-3}
[43]	X-ray diffraction of stacks of solution-grown crystals	72×10^{-3}	47×10^{-3}
[44]	From X-ray long period, bulk-grown, assuming crystallinity 40 to 50%		$41 \rightarrow 51 \times 10^{-3}$
Present work	Lamellar thickness from electron microscopy + from X-ray long period	$64 \pm 8 \times 10^{-3}$	$50 \pm 7 \times 10^{-3}$

Values of ΔH_m for HMF and LMF crystals are taken to be 1.98×10^8 and $\frac{3}{4} \times 1.98 \times 10^8$ J m^{-3}, respectively [45].

ΔH_m change with increasing pressure, because as has been pointed out in Section 1, both no change, increases and decreases have been observed for various polymers. If ΔH_m is assumed to be pressure-independent as is effectively observed for branched polyethylene [8, 19] then values of σ_e can be calculated. Values of $\sigma_e/\Delta H_m$ determined from the slopes of individual plots of the type shown in Fig. 11 range from 0.30 to 0.36 nm^{-1}. There is a suggestion of an increase but this cannot be stated categorically at this stage as the confidence limits on the slopes overlap. The average fold surface energies for LMF and HMF crystals are $50 \pm 7 \times 10^{-3}$ J m^{-2} and $64 \pm 8 \times 10^{-3}$ J m^{-2}. These values are compared with other published values in Table I. It can be seen that there is good agreement between the high-pressure values and the values for solution-grown, melt-grown in thin films, and bulk-grown crystals. This suggests that the crystals are of the same form in all cases. The values of σ_e calculated at each pressure range from 56 to 72×10^3 J m^{-2} and 43 to 54×10^3 J m^{-2} for HMF and LMF crystals, respectively. It is possible that σ_e may increase with increasing pressure of crystallization if ΔH_m is pressure-independent.

4. Conclusions

The melting temperatures of TPI crystals grown at 1 bar pressure increase by 15 K bar^{-1} as a function of melting pressure. This increase is a direct result of the changes in the thermodynamic parameters of the system as a function of pressure and is not due to crystal thickening. The measured equilibrium melting temperatures of both HMF and LMF TPI crystals, crystallized at pressure, increase by approximately 15 K kbar^{-1} over the pressure range 1 bar to 3 kbar. The increase in the equilibrium melting temperature can be attributed directly to the effect of pressure on the melting point and does not result from crystal thickening or increases in crystal perfection. Lamellar crystals of a given thickness melt at the same temperature, at 1 bar pressure, independent of the temperature or pressure of crystallization. The crystal thickness determined by both transmission electron microscopy and via long period measurements depend largely on the supercooling at all pressures.

The major effect of pressure on the thickness of TPI crystals grown at pressures of 1 bar to 3 kbar is clearly via the increase in the equilibrium melting temperature. Crystals of the same form

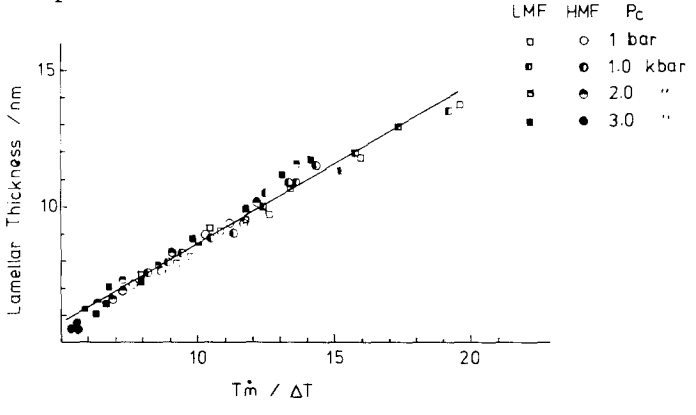

Figure 11 The lamellar thickness as a function of the ratio $T_m^0/\Delta T$.

grow over the whole pressure range by the same basic mechanism. At a given crystallization temperature the lamellar thickness decreases with increasing crystallization pressure. Crystal thickening is not observed and at no temperature do thick chain-extended type crystals grow.

Acknowledgements

The authors would like to thank the Science Research Council for financial support for this work. One of the authors, M. C. M. Cucarella would like to thank the Consejo de Desarrollo Cientifico y Humanistico of Venezuela for the maintenance grant that enabled this work to be carried out, and to thank the Department of Metallurgy and Materials Science of the Universidad Central de Venezuela for leave of absence. The authors would also like to thank Professor E. H. Andrews for helpful discussion and Dr D. A. Tod for help in apparatus design, computing work and general discussion throughout this work.

References

1. E. BAER and J. L. KARDOS, *J. Polymer Sci.* A3 (1965) 2827.
2. E. JENCKEL and H. RINKENS, *Z. Elektro. Chemie* **60** (1956) 970.
3. C. D. ARMENIADES and E. BAER, *J. Macromol. Sci.* **B1** (1967) 309.
4. K. MATSUSHIGE, S. HIRAKAWA and T. TAKEMURA, *Polymer J.* **3** (1972) 166.
5. L. R. FORTUNE and G. N. MALCOLM, *J. Phys. Chem.* **64** (1960) 934.
6. L. A. WOOD, N. BEKKEDAHL and R. E. GIBSON, *J. Chem. Phys.* **13** (1945) 475.
7. Y. MAEDA and H. KANETSUNA, *J. Polymer Sci. Polymer Phys. Ed.* **13** (1975) 637.
8. S. MATZUSKA, *J. Polymer Sci.* 57 (1962) 569.
9. M. YASUNIWA, C. NAKAFUKA and T. TAKEMURA, *Polymer J.* 4 (1973) 526.
10. K. TAKAMIZAWA, A. OHNA and Y. URABE, *ibid* 7 (1975) 342.
11. T. DAVIDSON and B. WUNDERLICH, *J. Polymer Sci. A-2* 7 (1969) 377.
12. W. B. PARKS and R. B. RICHARDS, *Trans. Faraday Soc.* **45** (1949) 203.
13. P. L. McGEER and H. C. DUUS, *J. Chem. Phys.* **20** (1952) 1813.
14. C. W. F. T. PISTORIUS, *Polymer* 5 (1964) 315.
15. M. TAMOYAMA, N. A. TERREL and H. EYRING, *Proc. Nat. Acad. Sci.* 57 (1967) 554.
16. W. W. DOLL and J. B. LANDO, *J. Macromol. Sci.* **4** (1970) 897.
17. T. KIJIMA, M. IMAMURA and N. KUSUMOTO, *Polymer* **17** (1976) 249.
18. S. GOGOLEWSKI and A. J. PENNINGS, *ibid.* **18** (1977) 654, 660, 667.
19. MARTHA C. M. CUCARELLA, Ph.D. Thesis, University of London (1978).
20. J. A. SAUER and K. D. PAE, *J. Appl. Phys.* **39** (1968) 4959.
21. B. E. WUNDERLICH, *J. Polymer Sci.* **A1** (1963) 1245.
22. D. V. REES and D. C. BASSETT, *ibid A2* 9 (1971) 385.
23. D. C. BASSETT and B. TURNER, *Phil. Mag.* **29** (1974) 285, 925.
24. T. HATAKEYANA, H. KANETSUNA, I. KANEDA, and J. HASHIMOTO, *J. Macromol. Sci. Phys.* **B10** (1974) 359.
25. D. C. BASSETT, *Polymer* **17** (1976) 460.
26. P. J. PHILLIPS and E. H. ANDREWS, *J. Polymer Sci.* **B10** (1972) 321.
27. *Idem, J. Polymer Sci. Phys.* **13** (1975) 1819.
28. C. K. L. DAVIES and ONG ENG LONG, *J. Mater. Sci.* **12** (1977) 2165.
29. *Idem. ibid.* **14** (1979) 2529.
30. E. G. LOVERING and D. C. WOODEN, *J. Polymer Sci. A-2* 9 (1971) 175.
31. C. W. BUNN, *Proc. Roy. Soc.* **A180** (1942) 40.
32. D. FISCHER, *Proc. Phys. Soc.* **66** (1953) 7.
33. E. H. ANDREWS, *Proc. Roy. Soc.* **A277** (1964) 562.
34. B. C. EDWARDS and P. J. PHILLIPS, *Polymer* **15** (1974) 491.
35. R. K. CRAWFORD, Ph.D. Thesis, Princeton University, New Jersey (1968).
36. J. R. WHITE, *J. Phys. D. Appl. Phys.* **10** (1977) 831.
37. C. G. VONK, *J. Appl. Cryst.* 4 (1971) 340.
38. B. CRIST and N. MOROSOFF, *J. Polymer Sci. Phys.* **11** (1973) 1023.
39. G. NATTA, P. CARRADINI and M. CESARI, *Rend. Accad. Naz. Lincei* **22** (1957) 11.
40. C. K. L. DAVIES and M. C. M. CUCARELL, *J. Mater. Sci.* **15** (1980) 1557.
41. J. D. HOFFMAN and J. I. LAURITZEN JR, *J. Res. Nat. Bur. Stand.* **65A** (1961) 297.
42. J. I. LAURITZEN JR, and J. D. HOFFMAN, *J. Appl. Phys.* 44 (1973) 4340.
43. A. KELLER and E. M. MARTUSCELLI, *Makromol. Chemie* **151** (1972) 189.
44. E. M. MARTUSCELLI, *ibid* **151** (1972) 159.
45. L. MANDELKERN, F. A. QUINN and D. E. ROBERTS, *J. Amer. Chem. Soc.* 78 (1956) 926.

Received 13 September and accepted 13 November 1979.